ACS APPLIED BIO MATERIALS

www.acsabm.org

Article

Gold Nanoparticles Are an Immobilization Platform for Active and Stable Acetylcholinesterase: Demonstration of a General Surface Protein Functionalization Strategy

Paul R. Handali and Lauren J. Webb*

Cite This: *ACS Appl. Bio Mater.* 2023, 6, 209–217

Read Online

ACCESS | Metrics & More | Article Recommendations | Supporting Information

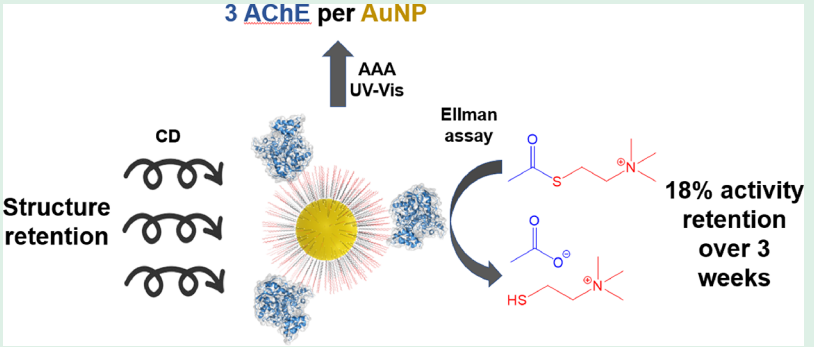

ABSTRACT: Immobilizing enzymes onto abiological surfaces is a key step for developing protein-based technologies that can be useful for applications such as biosensors and biofuel cells. A central impediment for the advancement of this effort is a lack of generalizable strategies for functionalizing surfaces with proteins in ways that prevent unfolding, aggregation, and uncontrolled binding, requiring surface chemistries to be developed for each surface−enzyme pair of interest. In this work, we demonstrate a significant advancement toward addressing this problem using a gold nanoparticle (AuNP) as an initial scaffold for the chemical bonding of the enzyme acetylcholinesterase (AChE), forming the conjugate AuNP−AChE. This can then be placed onto chemically and structurally distinct surfaces (e.g., metals, semiconductors, plastics, *etc.*), thereby bypassing the need to develop surface functionalization strategies for every substrate or condition of interest. Carbodiimide crosslinker chemistry was used to bind surface lysine residues in AChE to AuNPs functionalized with ligands containing carboxylic acid tails. Using amino acid analysis, we found that on average, 3.3 ± 0.1 AChE proteins were bound per 5.22 ± 1.25 nm AuNP. We used circular dichroism spectroscopy to measure the structure of the bound protein and determined that it remained essentially unchanged after binding. Finally, we performed Michaelis−Menten kinetics to determine that the enzyme retained 18.2 ± 2.0% of its activity and maintained that activity over a period of at least three weeks after conjugation to AuNPs. We hypothesize that structural changes to the peripheral active site of AChE are responsible for the differences in activity of bound AChE and unbound AChE. This work is a proof-of-concept demonstration of a generalizable method for placing proteins onto chemically and structurally diverse substrates and materials without the need for surface functionalization strategies.

KEYWORDS: *protein immobilization, acetylcholinesterase, activity retention, protein structure, protein quantification, gold nanoparticle functionalization*

INTRODUCTION

Proteins provide a broad range of functions ranging from enzymatic catalysis to electron transfer that can be exploited in devices for applications such as biosensing and biofuel cells, provided that they can be immobilized onto an abiological substrate such as metals, semiconductors, or nanomaterials. Despite the promise of this strategy, there are two significant hurdles that have prevented the advancement of new materials and devices beyond a few exceptional examples. The first challenge is that protein immobilization onto abiological materials often results in unfolding, aggregation, or other significant deformation of the biological molecule as it interacts with the artificial substrate. This in turn results in a decrease or complete loss of any function requiring a correct protein structure.[1−5] Uncontrolled binding also often results in

Received: October 3, 2022
Accepted: November 23, 2022
Published: December 12, 2022

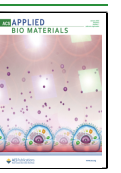

https://doi.org/10.1021/acsabm.2c00834
ACS Appl. Bio Mater. 2023, 6, 209–217

Scheme 1. Demonstration of the Use of NP−Protein Conjugates to Immobilize Proteins onto Different Substrates

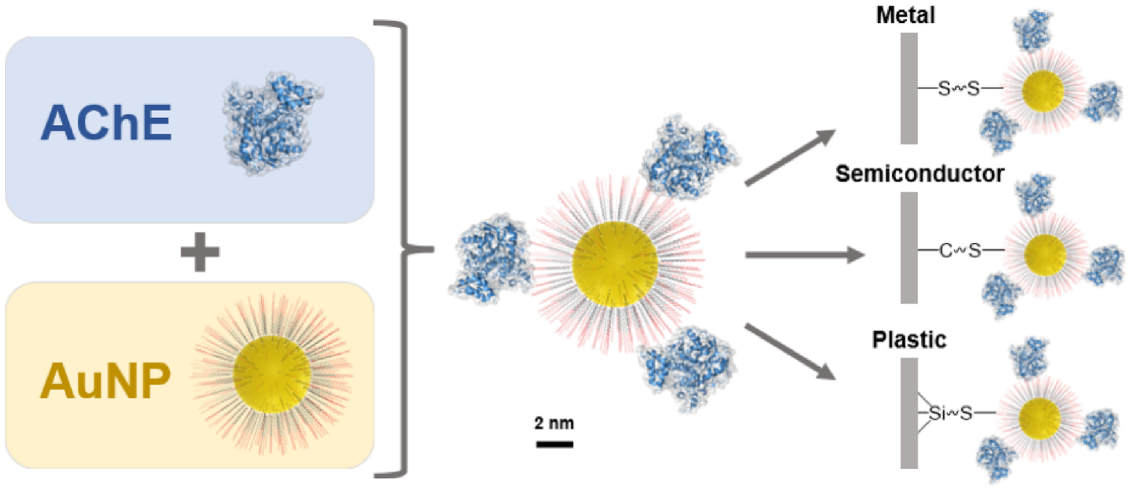

randomly oriented proteins, which can also decrease the activity by partially or fully blocking the functional region of interest such as an active site.[6−11] In response to this, there has been significant interest in developing surface functionalization strategies that optimize protein immobilization in a way that both controls the orientation within the material and maintains the integrity of the biomolecular structure and therefore function; common techniques include adsorption, covalent binding, and specific noncovalent binding such as DNA−DNA interactions or biotin−streptavidin conjugates.[4,12−15] This, however, highlights the second challenge: there is no generalizable immobilization strategy for integrating a protein into an abiological material, thus requiring unique methods be developed and characterized for each new enzyme−substrate pair investigated. To address both of these shortcomings, we are working toward using nanoparticles (NPs) as an initial protein immobilization platform to generate an NP−enzyme construct to address the first obstacle. This construct can then be easily immobilized onto a wide variety of surfaces such as metals, semiconductors, and plastics to address the second obstacle, as shown in Scheme 1. There are many reports of using NPs as an immobilization platform for proteins because these nanoscale materials have been shown to be useful for applications such as drug delivery, imaging, sensing, and catalysis.[16−23] Indeed, much work has gone into developing conjugation strategies[9,12,24,25] and characterizing interactions between the NP and the protein corona, a dense layer of proteins that often surround an NP in solution.[4] However, full characterization of protein−NP conjugates, such as quantifying the number of bound proteins, changes in biomolecular structure compared to solution, and how the presence of the surface itself affects activity or other function, can be challenging because of the presence of NP.[1] In this work, we focus on gold nanoparticles (AuNPs) as the immobilization platform, analyzing the structure, function, and amount of protein bound to the AuNP to address oversights in the characterization of proteins conjugated to a wide variety of NP materials.

The use of AuNPs as an initial scaffold presents several key advantages. AuNPs are straightforward to synthesize and characterize and have interesting optical and electronic properties that are particularly useful in areas such as sensing and catalysis.[16,26−28] Importantly for biomolecule applications, AuNPs can be easily solubilized in aqueous solution at physiological pH using capping ligands that prevent aggregation. In previous works, we reported on a water-stable peptide−AuNP conjugate using self-assembled monolayers (SAMs) of a mixture of hydroxy-terminated oligo-ethylene glycol (OEG) terminated alkylthiols (SH-C_n-OEG) and azide-terminated OEG alkyl thiols (SH-C_{11}-OEG-N_3) to cap the AuNPs. The azide-terminated moiety was then used to covalently bind a peptide to AuNPs using copper-catalyzed Huisgen cycloaddition ("click") chemistry.[29,30] This demonstrated that SH-C_n-OEG-capped AuNPs are robust to these reaction conditions in aqueous solution and when covalently bound to a peptide and thus can also potentially be used for binding to an entire protein.

We have previously studied the effects on the activity and structure of adsorbing a monolayer of the enzyme acetylcholinesterase (AChE) onto a planar gold surface, observing that although the enzyme retained approximately 10% of its activity, it subsequently maintained that activity over 100 days in buffer solution at 4 °C.[31] This was particularly striking when contrasted to the native aqueous enzyme, which was observed to become completely inactive after 6 days in the same buffer solution, demonstrating that immobilization onto a surface imparted stability on the structure and function of the enzyme. In the work reported here, we take a significant step to generalize this effort by demonstrating the immobilization of AChE on 5 nm AuNPs capped with carboxylic acid-tailed pegylated alkylthiols (AuNP−COOH). AChE is a serine hydrolase that hydrolyzes the neurotransmitter acetylcholine and is a particularly efficient enzyme, with a catalytic rate that approaches diffusion control, 10^9 M^{-1} s^{-1}.[32] AChE was covalently bound to AuNP−COOH using carbodiimide crosslinking chemistry to react the COOH groups on the AuNP surface with solvent-exposed lysine residues on AChE.[33,34] The resulting AuNP−AChE construct was then characterized by investigating the activity, the structure, and quantity of AChE bound per AuNP. We then determined the effects of covalent binding on the AChE by investigating changes in the activity and structure of the enzyme. Knowing the amount of AChE bound to AuNPs is critical to compare the activity of AChE when it is bound to the AuNP *versus* dissolved in solution. We demonstrate that this well-characterized protein−NP construct can serve as an initial building block toward the goal of developing a generalizable

https://doi.org/10.1021/acsabm.2c00834
ACS Appl. Bio Mater. 2023, 6, 209−217

strategy for immobilizing proteins on a wide variety of different chemical surfaces and substrates.

RESULTS AND DISCUSSION

Synthesis of AuNP−AChE. Prior to synthesis of AuNP−AChE, commercial AChE was purified by size exclusion chromatography.[35] The AuNPs used in this work were determined to have 4.7 ± 1.2 nm Au cores using transmission electron microscopy (TEM) (Figure S1A) and were functionalized with (11-mercaptoundecyl)tri(ethylene glycol)-carboxylic acid (SH-C_{11}-OEG_3-COOH) ligands. These AuNPs were readily soluble in aqueous solution and remained so after reaction with AChE, with no significant difference in Au core size before and after reaction (5.2 ± 1.3 nm) (Figure S1B). AChE was bound to AuNP−COOH by activating the COOH ligands with 1-ethyl-3-(3′-dimethyaminopropyl) carbodiimide HCl (EDC) and sulfo-*N*-hydroxysuccinimide (sulfo-NHS) to make them reactive to the lysine residues in AChE. While this strategy does not immobilize proteins onto an AuNP in a specific orientation, it is a reliable and simple attachment method that can potentially be used to bind most proteins to NPs since surface lysine residues are ubiquitous.[12] A control was run where AuNP−COOH was incubated with AChE without prior exposure to EDC/sulfo-NHS. Unbound AChE was then separated from the AuNP−AChE conjugates by centrifugation. Successful covalent binding of AChE to AuNP−COOH was confirmed using attenuated total reflectance infrared spectroscopy (ATR-IR) to monitor the appearance of amide I and amide II bands (carbonyl stretching and N−H bending of the amide backbone) at 1653 and 1550 cm^{-1}, respectively, which were indicative of the presence of protein.[36] Samples were concentrated using spin filters and then dropcast onto the ATR crystal. The spectra were normalized to the C−O stretch at 1120 cm^{-1} to account for peak height differences between runs. As can be seen in Figure 1, amide I and II bands were present in both the control and the sample, though the peaks in the sample were approximately three times more intense than those in the control. The presence of these peaks in the control indicated that the separation process did not completely remove the unbound protein, likely because it was adsorbed onto the AuNP. The presence of some adsorbed proteins likely conflates the amount of protein per AuNP and might convolute structural measurements; this is discussed extensively below. Nevertheless, these spectra demonstrate that introducing the activating agents increases the amount of protein on the AuNPs, showing that the protein was indeed covalently bound and that the AuNP−AChE conjugate was successfully synthesized.

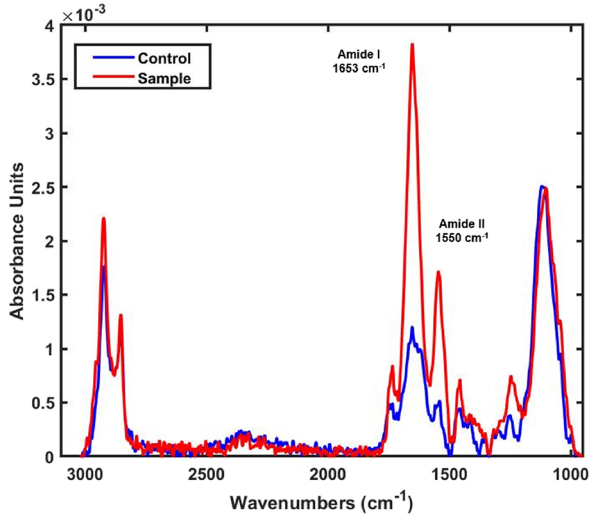

Figure 1. Infrared spectra of AuNPs reacted with AChE, where the control (blue) had no activating agent versus the sample (red), showing characteristic amide bands at 1653 and 1550 cm^{-1}. Spectra are normalized to the C−O stretch peak at 1120 cm^{-1}.

Quantifying the Number of AChE Bound per AuNP. The ratio of protein to AuNP in the AuNP−AChE was then determined using a modified amino acid analysis (AAA) procedure reported by Oliverio et al.[37] Accurately quantifying the number of bound enzymes per AuNP, whether or not they remained functional, was crucial for comparing the activity of AChE when bound to AuNP *versus* the native aqueous enzyme. It was also necessary to assess the structure of the AuNP-bound protein using circular dichroism(CD) spectroscopy (discussed below).[38] To perform this assay, the sample was digested in 6 M HCl at 110 °C for 24 h to hydrolyze the peptide bonds in the protein to generate free amino acids. The HCl was then evaporated and the hydrolysates reconstituted in pH 8.5 sodium bicarbonate buffer. The free amino acids were then derivatized with 2,4,6-trinitrobenzenesulfonic acid (TNBS), and the absorbance was measured at 420 nm. A calibration curve using known concentrations of AChE was constructed to relate the absorbance at 420 nm to the mass of AChE (Figure 2). The mass of protein in the AuNP−AChE samples was determined using linear regression, and the mass was used in turn to determine the average number of AChE per AuNP. For the AuNP−AChE samples, equivalent amounts of AuNP−COOH were hydrolyzed in HCl for background subtraction since AuNPs at high enough concentrations could contribute to background absorbance at 420 nm. Using this assay, it was determined that the AuNP−AChE conjugation resulted in 3.3 ± 0.1 AChE per AuNP. The geometric surface area of the AuNP available to bind to enzymes, calculated using the average NP radius previously determined by TEM, was approximately 26 nm^2. The largest diameter of the AChE catalytic unit is approximately 7 nm based on the crystal structure.[35] Given these dimensions, we determined that the

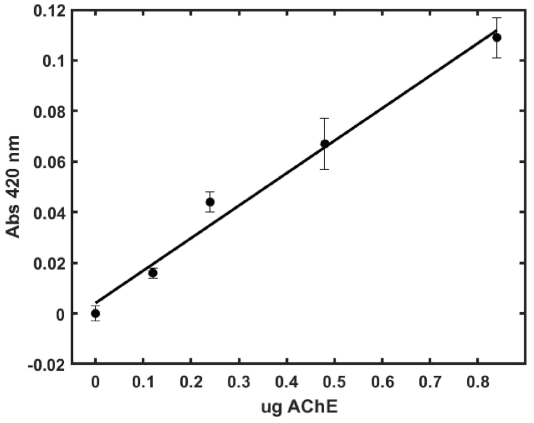

Figure 2. Calibration curve showing the relationship between mass of AChE and absorbance at 420 nm on samples that have been hydrolyzed in HCl for 24 h and derivatized with TNBS. Error bars indicate the standard deviation of three measurements.

https://doi.org/10.1021/acsabm.2c00834
ACS Appl. Bio Mater. 2023, 6, 209−217

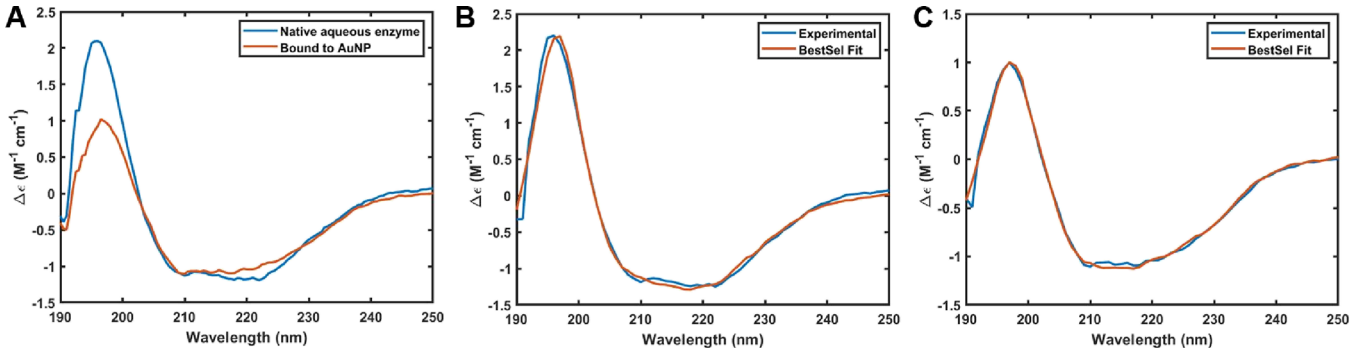

Figure 3. Representative CD spectra of AChE before and after covalent binding to AuNPs. (A) Overlaid spectra of AChE bound to AuNPs (orange) *versus* native aqueous AChE (blue). Spectra of (B) native aqueous AChE and (C) AuNP−AChE (blue) overlaid with their respective BestSel fits (red).

immobilized enzymes do not form a protein corona around the AuNP and that the enzymes are not overcrowded. A scale model of this is shown in the middle portion of Scheme 1. One limitation of the AAA assay is that it is an ensemble measurement and thus gives no insight into heterogeneous distribution of proteins per AuNP. AChE exists as a tetramer in solution,[35] so it is possible that there are AuNPs not bound to any AChE while others are bound to multiple sets of tetramers. Quantification of bound protein is an important characterization step that is often overlooked in the bio/abio literature. Indeed, despite the fact that the quantification of proteins is a relatively simple process in solution, it remains a challenge to routinely measure the number of bound proteins on NPs since the presence of NPs tends to complicate and interfere with the well-established protein quantification techniques.[39−42] The method demonstrated here significantly simplifies this characterization step and should be applicable for a wide variety of inorganic materials. In addition, these results also demonstrate that there is ample surface area on the AuNP left available to bind the conjugate to a macrosurface. This is important as it shows that it is plausible to use NP−protein conjugates as an initial binding step to binding proteins to surfaces.

Secondary Structure of AChE Bound to AuNPs. Protein function is intimately related to its structure, and protein binding to NPs has been shown to have an effect on the protein's structure.[2,12,43−45] It was therefore important to characterize the structure of the bound protein to determine whether any observed decrease in function was potentially a result of unfolding or other deleterious structural change of the protein once in contact with the AuNP. To this end, we turned to CD spectroscopy to determine the secondary structure of AChE based on the UV adsorption of circularly polarized light by the protein's amide bonds.[1,29,30,46−50] CD was performed on solution-phase AChE and the AuNP−AChE construct to observe the effect of covalent binding on the secondary structure of the protein with solvent blanks (10 mM phosphate buffer) for background subtraction. The spectra were fit using the online deconvolution server BestSel to determine conformational fractions.[38,51] As shown in Figure 3A, qualitatively, the CD spectra of bound *versus* unbound AChE were very similar, with the only notable differences being a slightly lower dip at 222 nm and a taller peak at 195 nm for unbound AChE. These minimal changes were reflected in spectral deconvolution (Table 1) to determine the conformational fractions. The spectral deconvolution fits compared to the CD spectra for bound and unbound AChE are shown in Figure 3B,C respectively. The α-helical character (8.4% *versus* 11.6%) and slightly increased β-sheet and β-turn character (30.7% *versus* 25.2 and 14% *vs* 12% respectively) remain largely the same between the bound and native aqueous enzyme, respectively. These spectra demonstrate that covalent binding of AChE on AuNPs using EDC/NHS cross-linker chemistry does not have a significant effect on the structure of the protein. This information is important for disentangling potential contributions to differences in the activity of the bound protein.

Table 1. Percentage of Structural Elements of AuNP−AChE and Native Aqueous AChE as Determined by BestSel Deconvolution of the Respective CD Spectra

structural element	AuNP−AChE	AChE
α-helix	8.4	11.6
β-sheet	30.7	25.2
β-turn	14	12
others	46.9	51.1

Measuring the Activity of AuNP−AChE. To determine the effect of binding on the function of AChE, an activity assay was performed on the AuNP−AChE construct to compare function to the native aqueous AChE. This assay, developed by Ellman,[52] measures the activity of AChE by monitoring the amount of a thioester variant of AChE's natural substrate acetylcholine, acetylthiocholine (ATCh), hydrolyzed by AChE into thiocholine in a specific time frame. Ellman's reagent, 5,5-dithio-bis-(2-nitrobenzoic acid) (DTNB), was added to react with thiocholine and released 1 equiv of thio-2-nitrobenzoic acid (TNB) anion. The absorbance of the TNB anion could then be measured at 412 nm to determine the amount of ATCh hydrolyzed per second by AChE. After adding all reagents, the reaction was quenched with the addition of 2% sodium dodecyl sulfate (SDS) after 2 min and the absorbance at 412 nm measured. The activity of AuNP−AChE was compared to the activity of the control (AChE reacted with AuNPs in the absence of EDC/NHS), where equivalent amounts of AuNPs were added for both the sample and control. The activity of AChE was measured in units of specific activity (U), which is defined as the μmol substrate hydrolyzed per min. As shown in Figure 4A, the sample is significantly more active than the control, 0.150 ± 0.006 U *versus* (0.24 ± 0.08) × 10^{-3} U. This indicates two things. First, it suggests that the amount of non-covalently bound AChE previously observed using ATR-IR discussed earlier is negligible and that the centrifugation is sufficient to separate AuNP−AChE

https://doi.org/10.1021/acsabm.2c00834
ACS Appl. Bio Mater. 2023, 6, 209−217

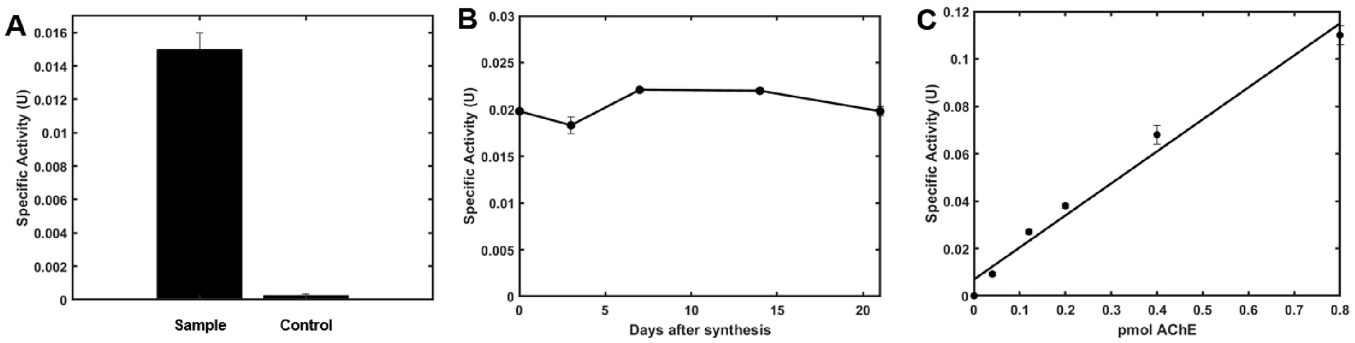

Figure 4. Activity measurements of native aqueous AChE and bound to AuNPs measured in units of specific activity. (A) Specific activity of reaction product of AuNPs and AChE compared to the control where the activating agent EDC/sulfo-NHS was excluded from the reaction mixture. (B) Activity retention of AuNP−AChE over time stored at 4 °C. The same sample was measured over the course of three weeks. (C) Calibration curve relating specific activity to the amount of AChE in pmol. Error bars indicate the standard deviation of three measurements.

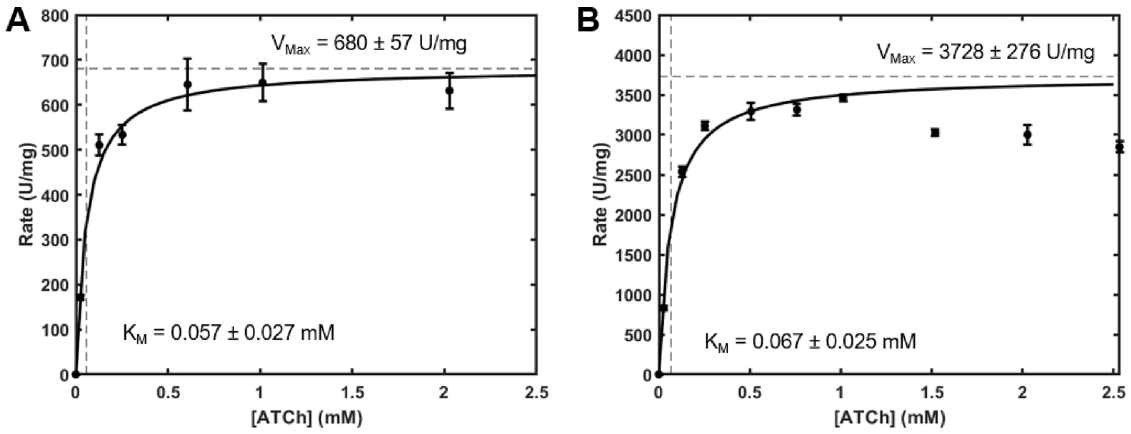

Figure 5. Michaelis−Menten kinetics plots of (A) AuNP−AChE and (B) native aqueous AChE relating the specific activity normalized by mass of AChE to the concentration of the substrate ATCh. Error bars in the plots indicate the standard deviation of three measurements. Error in coefficients are 95% confidence intervals.

from unbound AChE. It also shows that the AAA assay described above quantified mostly covalently bound proteins as opposed to proteins simply adsorbed on the AuNP. Second, it demonstrates that the AChE remains active once covalently bound to the AuNP. The fact that the protein retains its function is unsurprising given the results from CD that demonstrated that the enzyme structure remains mostly unchanged. We measured the activity of AuNP−AChE over time to monitor the stability of the bound protein after synthesis; this is shown in Figure 4B. The activity remained the same over the course of three weeks (after which the experiment was ended), demonstrating that binding to the AuNP imparted stability on the enzyme. We have previously reported that native aqueous AChE completely loses activity after 6 days of storage at 4 °C but remains stable when adsorbed onto a flat macroscopic Au surface.[31] The data presented in Figure 4B corroborates the observation that immobilization onto a scaffold of some kind, regardless of its size, imparts stability on the enzyme's function. This is significant since it shows that the act of immobilizing proteins onto a platform is not only key to integrating proteins into inorganic materials but is also in fact beneficial to the stability and function of any device using this strategy over time.

To determine the extent of AChE's retention of activity, the number of active AChE's per AuNP must be measured. We used Ellman's assay described above to determine the number of active AChE proteins per AuNP by constructing a calibration curve that relates the activity to the amount of protein, seen in Figure 4C. Linear regression was applied to determine that on average, there were 0.36 ± 0.04 active AChE proteins per AuNP. This number was divided by the number of AChE per AuNP that was measured by AAA (3.3 ± 0.1) to find that 10.9 ± 1.3% of bound proteins remained active. It is important to remember that this result is based on ensemble measurements and thus cannot distinguish between all AChE present in the sample performing at 10.9% of their expected capacity *versus* 10.9% of AChE molecules being 100% active. This comparison demonstrates that covalent binding does indeed have a significant effect on the function of the protein despite having a minimal effect on the structure of the protein as discussed earlier. The reduction of the protein's activity is likely due to a combination of some structural changes and the orientation of the bound protein. One way to potentially improve the activity retention is to control the orientation of the bound protein using site-specific conjugation. Many such strategies have been developed such as biotin−streptavidin conjugates[12,53,54] and bio-orthogonal reactions such as tetrazine ligation and azide-alkyne click chemistry.[55,56] These strategies could prove difficult for use in AChE however, as they require mutations to the protein and recombinant AChE expression is difficult.[57] It is important to note, however, that despite the dramatic reduction in the enzyme's activity, this AuNP−AChE construct can still be useful for different applications. For example, AChE is inhibited by organo-

https://doi.org/10.1021/acsabm.2c00834
ACS Appl. Bio Mater. 2023, 6, 209−217

phosphates common in pesticides and chemical nerve agents and thus loses activity in the presence of these compounds.[58−60] This is a mechanism that can be exploited for sensing of these organophosphates using the AuNP−AChE conjugates bound to a surface.

Further insights into the relationship between the changes in structure and the activity were investigated using Michaelis−Menten kinetics, which measures enzyme activity as a function of substrate concentration. This was performed on both the AuNP−AChE construct and native aqueous AChE.[31,61] The data were fit to the Michaelis−Menten model (eq 1):

$$\nu = \frac{V_{\mathrm{Max}}[S]}{K_{\mathrm{M}} + [S]} \quad (1)$$

where ν is the initial rate of reaction, V_{Max} is the maximum achievable rate, $[S]$ is the concentration of the substrate, and K_{M} is the Michaelis constant, which is equal to $[S]$ at $(1/2)$ V_{Max}.[62] The activity is normalized by the amount of protein in the sample resulting in an activity unit of U mg^{-1}, which allows for a direct comparison to be made between bound AChE and native aqueous AChE. These results are shown in Figure 5. For both the native aqueous and the bound AChE, the increase in activity with respect to substrate concentration was linear until saturated at high concentrations of ATCh. However, there were several noteworthy differences between AuNP−AChE and unbound AChE. The V_{Max} of AuNP−AChE was significantly lower at 680 ± 57 U mg^{-1} (Figure 5A) *versus* the 3728 ± 276 U mg^{-1} of unbound AChE (Figure 5B). Taking the ratio of V_{Max} of AuNP−AChE to that of unbound AChE resulted in an 18.2 ± 2.0% retention of activity for AChE once it was covalently bound to AuNPs; this was slightly higher than the 10.9% activity retention discussed previously, but the values are comparable. Another notable difference was the activity of AChE at high concentrations of substrate. Native aqueous AChE exhibited a steady decrease in activity at higher concentrations of substrate as a result of substrate inhibition (Figure 5B).[61] However, this was not the case for AChE once bound to AuNPs (Figure 5A); once the activity of AuNP−AChE reached V_{Max}, it plateaued and did not show evidence of substrate inhibition as $[S]$ increased. Finally, the K_{M} of AuNP−AChE (0.057 ± 0.027 mM, Figure 5A) was similar to that of unbound AChE (0.067 ± 0.025 mM, Figure 5B). This indicates that the affinity of the protein for the substrate remains mostly the same once bound to AuNPs.

The explanations for both of these observations are likely related to changes in the structure of AChE once bound to the AuNP and the orientation of the enzyme relative to the AuNP substrate. The observation that points to a possible explanation is the lack of substrate inhibition in AuNP−AChE. The mechanism of substrate inhibition for AChE has been explored in depth and can provide insights into structural changes occurring in the bound enzyme that are also consistent with the lower V_{Max}.[63] AChE has two locations where the substrate can potentially bind (shown in Figure 6): the catalytic anionic site (CAS) and the peripheral anionic site (PAS).[63−65] The CAS, which is where substrate hydrolysis occurs, is located toward the bottom of the active site gorge, whereas the PAS is located toward the mouth of the active site gorge. At high concentrations, substrate binding to the PAS causes allosteric changes that have been shown to have inhibitory effects on the activity of AChE.[61,64] Since AuNP−AChE does not exhibit this substrate inhibition, it is possible that the substrate is unable to bind to the PAS either due to slight unfolding at the mouth of the active site gorge or the protein is oriented on the AuNP in a way that blocks substrate access to the PAS. However, at lower substrate concentrations, substrate binding to the PAS has also been shown to increase the rate of catalysis since the PAS can shuttle substrate molecules into the active site gorge.[66] Therefore, if the PAS in the AuNP−AChE construct is indeed prevented from binding to the substrate, this could explain the overall lower V_{Max} observed in the substrate-bound AChE. One way to test this hypothesis would be to observe the binding of the bound AChE to substrates that are specific to the PAS. One such substrate is thioflavin T, which is a fluorescent ligand that binds specifically to the PAS and has enhanced fluorescence when bound.[66] If the PAS is indeed inaccessible for substrate binding once bound to the AuNP, we would expect to see no change in the fluorescence of thioflavin T when added together with the AuNP−AChE. This, however, highlights a significant limitation of using a AuNP-based platform; this assay, and indeed every assay measuring binding to the PAS, has been reported for the native aqueous AChE. The presence of AuNPs will significantly complicate this characterization since AuNPs are strong quenchers of fluorescence.[41,67] Developing assays that are compatible with the AuNP is a significant thrust of future work, both in our laboratory and elsewhere.

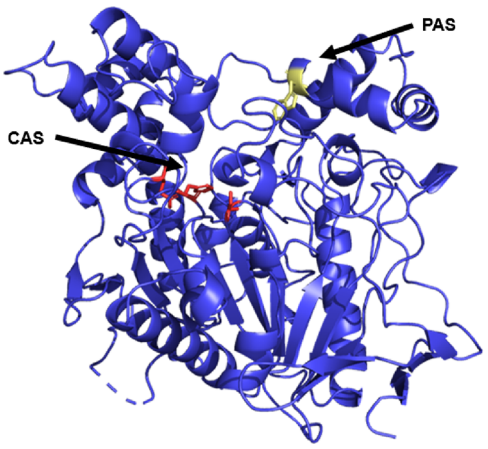

Figure 6. Crystal structure of electric eel AChE (PDB: 1EEA) showing the locations of the CAS and PAS. The residues of the catalytic triad in the CAS (Glu 327, His 440, and Ser 200) and the key residue in the PAS (Trp 279) are highlighted in red and yellow, respectively.

SUMMARY AND CONCLUSIONS

In this work, we covalently attached AChE to functionalized AuNPs using carbodiimide crosslinking chemistry to synthesize AuNP−AChE conjugates. These conjugates were then thoroughly characterized to determine the amount, structure, and activity of the bound protein. All of these metrics were compared to unbound AChE to determine the effects of covalent binding to the functionalized AuNP on the structure and function of AChE. It was determined with amino acid analysis that on average, 3.3 ± 0.1 AChE were bound per AuNP and that the structure of the protein remains largely intact after binding using CD spectroscopy. Using activity and kinetics assays, bound AChE retained 10.9 ± 1.3% of its activity and exhibited no substrate inhibition when compared to unbound AChE. We also observed that the protein retains

https://doi.org/10.1021/acsabm.2c00834
ACS Appl. Bio Mater. 2023, 6, 209−217

the same level of activity three weeks after binding to the AuNP, demonstrating that immobilization imparted stability on the enzyme activity. The mechanism for this promising observation is currently under investigation. We propose that the changes in activity were likely the result of inability of the substrate to bind to the PAS at the mouth of the active site gorge either due to a combination of the orientation of the protein with respect to the AuNP and minor structural changes to the protein. Although the protein lost a significant amount of its activity as a result of binding, we demonstrate that we can fully characterize the protein−AuNP conjugate, which we can then immobilize onto different kinds of surfaces. Future work will focus on binding this AuNP−AChE conjugate to surfaces such as silicon, plastics, and metals as a logical next step as we have shown that there is ample surface area on the AuNP available to bind to a macrosurface. This will then demonstrate a first proof-of-concept toward a generalizable strategy for immobilizing proteins onto different kinds of surfaces.

EXPERIMENTAL SECTION

Materials and Chemicals. H_2SO_4, NaOH, NaCl, Na_2HPO_4, 2-(*N*-morpholino) ethanesulfonic acid (MES), 4-(2-hydroxyethyl)-1-piperazineethanesulfonic acid (HEPES), ethanol, and toluene were purchased from Fisher Scientific. Acetylthiocholine iodide, Type VI-S acetylcholinesterase from electric eel (*Electrophorus electricus*), 1-ethyl-3-(3′-dimethyaminopropyl) carbodiimide HCl (EDC), sulfo-*N*-hydroxysuccinimide (sulfo-NHS), 4-(dimethylamino) pyridine (DMAP), tetraocetylammonium bromide (TOAB), picrylsulfonic acid, $HAuCl_4$, $NaBH_4$, anhydrous $MgSO_4$, and Amicon Ultra 0.5 mL 30 kDa and 100 kDa molecular weight cutoff filters were purchased from Millipore Sigma. SH-C_{11}-PEG_3-COOH was purchased from Biochempeg.

AuNP−COOH Synthesis. AuNPs capped with SH-C_{11}-PEG_3-COOH ligands (AuNP−COOH) were synthesized according to a previously published procedure.[30,68] Briefly, an aqueous solution of $HAuCl_4$ (0.142 M, 1 mL) was added to a solution of TOAB (0.030 M, 10 mL) in toluene and stirred for 30 min. An aqueous solution of $NaBH_4$ (1.5 M, 1 mL) was then added to the reaction mixture and allowed to stir overnight. The reaction mixture was then transferred to a separation funnel, and the aqueous layer was discarded. The organic phase was then washed with H_2SO_4 (0.1 M, 10 mL), NaOH (0.1 M, 10 mL), and deionized water (10 mL) sequentially. This washing procedure was repeated three times. An aqueous solution of DMAP (0.1 M, 10 mL) was added to the separation funnel and was shaken vigorously for 5 min. The two phases were allowed to separate as the AuNPs transferred from the organic phase into the aqueous phase, resulting in DMAP-capped AuNPs (AuNP−DMAP). The aqueous layer was then collected and the organic layer discarded. Absorbance at 506 nm was used to measure the concentration of the AuNPs (ε = 8.5×10^6 M^{-1} cm^{-1}).[69]

A solution of SH-C_{11}-PEG_3-COOH (10 mM, 700 μL) in ethanol was added to the AuNP−DMAP (1.15 μM, 1.5 mL) and left overnight at room temperature. The resulting AuNP−COOH was then purified from free ligands by centrifugation in Amicon Ultra 0.5 mL 30k spin filters at 14,000*g* for 8 min. The AuNPs were then resuspended in pH 5 10 mM MES buffer. This process was repeated eight times. The resulting AuNP−COOH in pH 5 MES buffer were then stored at room temp in the dark until use. Transmission electron microscopy (TEM, JEOL 2010F) was used to determine the size distribution of the AuNPs (n = 200).

AChE Purification. AChE was purified using a previously reported procedure.[31,35] Briefly, 6.5 mg of AChE solid was dissolved in 650 μL of running buffer (10 mM phosphate, 400 mM NaCl, pH 7) and injected into a Superdex 200 size exclusion column. AChE was collected as a single peak and concentrated with Amicon Ultra 0.5 mL 10k spin filters at 14,000*g*. The AChE was then solvent exchanged into 10 mM pH 8 HEPES buffer and used immediately for conjugation with AuNP−COOH.

Synthesis of AuNP−AChE. To a solution of AuNP−COOH in 10 mM pH 5 MES buffer (0.5 μM, 125 μL) was added a solution of 47.9 mg EDC (0.25 mmol) and 108 mg sulfo-NHS (0.5 mmol) in 250 μL of 10 mM pH 5 MES buffer. The reaction mixture was shaken at 1000 rpm for 15 min at room temperature, after which unreacted EDC/sulfo-NHS was separated from the AuNPs using Amicon Ultra 0.5 mL 100 kDa spin filters at 21,000*g*. The AuNPs were resuspended in 10 mM pH 8 HEPES buffer, and this process was repeated three times. The resulting sulfo-NHS-activated AuNP−COOH was then added to 250 μL of 1 mg/mL^{-1} pure AChE solution and was shaken at 1000 rpm at 4 °C overnight, resulting in AuNP−AChE conjugates. To separate out the unreacted AChE, the reaction mixture was spun at 60,000*g* for 20 min, which resulted in the AuNP−AChE collected at the bottom of the centrifuge tube. The supernatant was then removed and the AuNP−AChE resuspended in 150 μL of 10 mM pH 7 phosphate buffer. This process was repeated eight times. The AuNP−AChE was then used immediately for activity and structure measurements. The solution was stored at 4 °C for stability measurements over three weeks.

Activity Measurements. The activity of native aqueous AChE and AChE bound to AuNPs was measured using a spectroscopic assay developed by Ellman.[52] This assay substitutes the native substrate of AChE, acetylcholine, with a thioester variant, acetylthiocholine (ATCh). AChE hydrolyzes the ATCh into thiocholine and acetate, after which the thiocholine is labeled with DTNB. The reaction results in the release of the thio-2-nitrobenzoic acid (TNB) anion, which absorbs strongly at 412 nm ($\varepsilon = 1.36 \times 10^4$ M^{-1} cm^{-1}) and was used as a measure of ATCh hydrolyzed over a specific time.

To perform this assay, 3 mL of 100 mM pH 8 phosphate buffer was added to a disposable cuvette followed by 20 μL of 0.01 M DTNB solution in 100 mM pH 7 phosphate buffer and 0.018 M sodium bicarbonate. To this was added 2 μL of 0.056 μM AuNP−AChE followed by 5 μL of 0.075 M ATCh. The reaction was quenched with 100 μL of 2% SDS to inactivate the AChE after 2 min, after which measurements at 412 nm were taken. Each assay was performed in triplicate.

Attenuated Total Internal Reflection Fourier-Transform Infrared Spectroscopy (ATR-FTIR). ATR-FTIR was used to analyze the ligand shell of the AuNP−COOH and to confirm AChE binding. These measurements were collected on a Vertex 70 FTIR (Bruker) with a liquid N_2-cooled HgCdTe (MCT) detector and a Ge ATR accessory (Harrick). A solution of 0.50 μM AuNP−COOH or 0.056 μM AuNP−AChE in deionized water was concentrated using Amicon Ultra 0.5 mL 100k spin filters, 10 μL of which was then dropcast onto the ATR crystal to dry. A total of 500 scans was taken for each measurement at 4 cm^{-1} resolution. The spectra of a clean ATR crystal were used for background subtraction. Baseline corrections were performed using OPUS software (Bruker). All spectra were normalized to the C−O stretching band at 1120 cm^{-1}.

Circular Dichroism (CD) Spectroscopy. CD was used to measure the secondary structure of native aqueous AChE and bound to AuNPs. Spectra were measured on a JASCO J-815 CD spectrometer (JASCO). A 1 mm pathlength quartz cuvette was used for all measurements. Spectra were recorded from 260 to 190 nm with the bandwidth set to 1 nm, 4 s response time, and 50 nm min^{-1} scan rate. A blank spectrum of 10 mM pH 7.5 phosphate buffer was used for background subtraction. Spectra for AuNP−AChE were obtained from an average of 100 scans, while spectra for native aqueous AChE were obtained from an average of 10 scans.

Amino Acid Analysis (AAA). A modified AAA protocol reported by Oliverio *et al.* was used to determine the number of AChE per AuNP.[37] A calibration curve was created using varying concentrations of pure AChE in solution. To a 50 μL solution of 0.056 μM AuNP−AChE was added 100 μL of 6 M HCl. The resulting solution was left in a heating block at 110 °C for 24 h. The vials were then opened and left at 110 °C to evaporate the HCl. The dried samples were then resuspended in 100 μL of 100 mM pH 8.5 sodium bicarbonate, which was then pipetted into a clear flat-bottom 96-well microplate. To this

https://doi.org/10.1021/acsabm.2c00834
ACS Appl. Bio Mater. 2023, 6, 209−217

was added 50 μL of 0.01% TNBS solution in 100 mM sodium bicarbonate. The microplate was then kept at 37 °C for 2 h, after which 50 μL of 10% SDS was added. Absorbance at 420 nm was then read on a Synergy H4 Hybrid Multi-Mode Microplate Reader (BioTek). Each assay was performed in triplicate.

■ ASSOCIATED CONTENT

Supporting Information

The Supporting Information is available free of charge at https://pubs.acs.org/doi/10.1021/acsabm.2c00834.

TEM images of AuNP−COOH and AuNP−AChE (PDF)

■ AUTHOR INFORMATION

Corresponding Author

Lauren J. Webb − *Department of Chemistry, Texas Materials Institute, and Interdisciplinary Life Sciences Program, The University of Texas at Austin, Austin, Texas 78712-1224, United States;* orcid.org/0000-0001-9999-5500; Email: lwebb@cm.utexas.edu

Author

Paul R. Handali − *The University of Texas at Austin, Austin, Texas 78712-1224, United States*

Complete contact information is available at: https://pubs.acs.org/10.1021/acsabm.2c00834

Notes

The authors declare no competing financial interest.

■ ACKNOWLEDGMENTS

This work was supported by the U.S. Army Research Office (Grant No. W911NF-17-1-0089), National Science Foundation (Grant Nos. CHE-1807215 and CHE-2203414), and the Robert. A. Welch Foundation (Grant No. F-1722). We gratefully acknowledge the UT-Austin Texas Materials Institute and the UT-Austin Texas Institute for Drug and Diagnostic Discovery for the use of their facilities.

■ REFERENCES

(1) Sapsford, K. E.; Tyner, K. M.; Dair, B. J.; Deschamps, J. R.; Medintz, I. L. Analyzing Nanomaterial Bioconjugates: A Review of Current and Emerging Purification and Characterization Techniques. *Anal. Chem.* **2011**, *83*, 4453−4488.

(2) Woods, K. E.; Perera, Y. R.; Davidson, M. B.; Wilks, C. A.; Yadav, D. K.; Fitzkee, N. C. Understanding Protein Structure Deformation on the Surface of Gold Nanoparticles of Varying Size. *J. Phys. Chem. C* **2016**, *120*, 27944−27953.

(3) Aubin-Tam, M. E.; Hamad-Schifferli, K. Structure and Function of Nanoparticle-Protein Conjugates. *Biomed. Mater.* **2008**, *3*, No. 034001.

(4) Mahmoudi, M.; Lynch, I.; Ejtehadi, M. R.; Monopoli, M. P.; Bombelli, F. B.; Laurent, S. Protein - Nanoparticle Interactions: Opportunities and Challenges. *Chem. Rev.* **2011**, *111*, 5610−5637.

(5) Sethuraman, A.; Vedantham, G.; Imoto, T.; Pryzbycien, T.; Belfort, G. Protein Unfolding at Interfaces: Slow Dynamics of α-Helix to β-Sheet Transition. *Proteins: Struct., Funct., Bioinf.* **2004**, *56*, 669−678.

(6) Liu, Y.; Yu, J. Oriented Immobilization of Proteins on Solid Supports for Use in Biosensors and Biochips: A Review. *Microchim. Acta* **2016**, *183*, 1−19.

(7) Trilling, A. K.; Beekwilder, J.; Zuilhof, H. Antibody Orientation on Biosensor Surfaces: A Minireview. *Analyst* **2013**, *138*, 1619−1627.

(8) Hitaishi, V.; Clement, R.; Bourassin, N.; Baaden, M.; de Poulpiquet, A.; Sacquin-Mora, S.; Ciaccafava, A.; Lojou, E. Controlling Redox Enzyme Orientation at Planar Electrodes. *Catalysts* **2018**, *8*, 1−38.

(9) Yong, K. W.; Yuen, D.; Chen, M. Z.; Porter, C. J. H.; Johnston, A. P. R. Pointing in the Right Direction: Controlling the Orientation of Proteins on Nanoparticles Improves Targeting Efficiency. *Nano Lett.* **2019**, *19*, 1827−1831.

(10) Ruiz, G.; Tripathi, K.; Okyem, S.; Driskell, J. D. pH Impacts the Orientation of Antibody Adsorbed onto Gold Nanoparticles. *Bioconjugate Chem.* **2019**, *30*, 1182−1191.

(11) Meissner, J.; Wu, Y.; Jestin, J.; Shelton, W. A.; Findenegg, G. H.; Bharti, B. PH-Induced Reorientation of Cytochrome c on Silica Nanoparticles. *Soft Matter* **2019**, *15*, 350.

(12) Sapsford, K. E.; Algar, W. R.; Berti, L.; Gemmill, K. B.; Casey, B. J.; Oh, E.; Stewart, M. H.; Medintz, I. L. Functionalizing Nanoparticles with Biological Molecules: Developing Chemistries That Facilitate Nanotechnology. *Chem. Rev.* **2013**, *113*, 1904−2074.

(13) Hlady, V.; Buijs, J. Protein Adsorption on Solid Surfaces. *Curr. Opin. Biotechnol.* **1996**, *7*, 72−77.

(14) Rusmini, F.; Zhong, Z.; Feijen, J. Protein Immobilization Strategies for Protein Biochips. *Biomacromolecules* **2007**, *8*, 1775−1789.

(15) Mohamad, N. R.; Haziqah, N.; Marzuki, C.; Buang, N. A.; Wahab, R. A. An Overview of Technologies for Immobilization of Enzymes and Surface Analysis Techniques for Immobilized Enzymes. *Biotechnol. Biotechnol. Equip.* **2015**, *29*, 205−220.

(16) Elahi, N.; Kamali, M.; Baghersad, M. H. Recent Biomedical Applications of Gold Nanoparticles: A Review. *Talanta* **2018**, *184*, 537−556.

(17) Spicer, C. D.; Jumeaux, C.; Gupta, B.; Stevens, M. M. Peptide and Protein Nanoparticle Conjugates: Versatile Platforms for Biomedical Applications. *Chem. Soc. Rev.* **2018**, *47*, 3574−3620.

(18) Malekzad, H.; Sahandi Zangabad, P.; Mirshekari, H.; Karimi, M.; Hamblin, M. R. Noble Metal Nanoparticles in Biosensors: Recent Studies and Applications. *Nanotechnol. Rev.* **2017**, *6*, 301−329.

(19) You, C.; Agasti, S. S.; De, M.; Knapp, M. J.; Rotello, V. M. Modulation of the Catalytic Behavior of r -Chymotrypsin at Monolayer-Protected Nanoparticle Surfaces. *J. Am. Chem. Soc.* **2006**, *128*, 14612−14618.

(20) Yu, R.; Wang, R.; Wang, Z.; Zhu, Q.; Dai, Z. Applications of DNA-Nanozyme-Based Sensors. *Analyst* **2021**, *146*, 1127−1141.

(21) Manzano, M.; Vallet-Regí, M. Mesoporous Silica Nanoparticles for Drug Delivery. *Adv. Funct. Mater.* **2020**, *30*, No. 1902634.

(22) Mitchell, M. J.; Billingsley, M. M.; Haley, R. M.; Wechsler, M. E.; Peppas, N. A.; Langer, R. Engineering Precision Nanoparticles for Drug Delivery. *Nat. Rev. Drug Discovery* **2021**, *20*, 101−124.

(23) Hong, S.; Choi, D. W.; Kim, H. N.; Park, C. G.; Lee, W.; Park, H. H. Protein-Based Nanoparticles as Drug Delivery Systems. *Pharmaceutics* **2020**, *12*, 604.

(24) Zheng, M.; Huang, X. Nanoparticles Comprising a Mixed Monolayer for Specific Bindings with Biomolecules †. *J. Am. Chem. Soc.* **2004**, *126*, 12047−12054.

(25) Bayraktar, H.; You, C.-C.; Rotello, V. M.; Knapp, M. J. Facial Control of Nanoparticle Binding to Cytochrome C. *J. Am. Chem. Soc.* **2007**, *129*, 2732−2733.

(26) Zhao, P.; Li, N.; Astruc, D. State of the Art in Gold Nanoparticle Synthesis. *Coord. Chem. Rev.* **2013**, *257*, 638−665.

(27) Daniel, M.-C.; Astruc, D. Gold Nanoparticles: Assembly, Supramolecular Chemistry, Quantum-Size-Related Properties, and Applications toward Biology, Catalysis, and Nanotechnology. *Chem. Rev.* **2004**, *104*, 293−346.

(28) Astruc, D. Introduction: Nanoparticles in Catalysis. *Chem. Rev.* **2020**, *120*, 461−463.

(29) Wilder, L. M.; Fies, W. A.; Rabin, C.; Webb, L. J.; Crooks, R. M. Conjugation of an α-Helical Peptide to the Surface of Gold Nanoparticles. *Langmuir* **2019**, *35*, 3363−3371.

(30) Wilder, L. M.; Handali, P. R.; Webb, L. J.; Crooks, R. M. Interactions between Oligoethylene Glycol-Capped AuNPs and Attached Peptides Control Peptide Structure. *Bioconjugate Chem.* **2020**, *31*, 2383−2391.

(31) Correira, J. M.; Webb, L. J. Formation and Characterization of a Stable Monolayer of Active Acetylcholinesterase on Planar Gold. *Langmuir* **2022**, *38*, 3501−3513.
(32) Stroppolo, M. E.; Falconi, M.; Caccuri, A. M.; Desideri, A. Superefficient enzymes. *Cell. Mol. Life Sci.* **2001**, *58*, 1451−1460.
(33) Sehgal, D.; Vijay, I. K. A Method for the High Efficiency of Water-Soluble Carbodiimide-Mediated Amidation. *Anal. Biochem.* **1994**, *218*, 87−91.
(34) Park, C.; Vo, C. L.-N.; Kang, T.; Oh, E.; Lee, B.-J. New Method and Characterization of Self-Assembled Gelatin − Oleic Nanoparticles Using a Desolvation Method via Carbodiimide / N-Hydroxysuccinimide (EDC / NHS) Reaction. *Eur. J. Pharm. Biopharm.* **2015**, *89*, 365−373.
(35) Bourne, Y.; Grassi, J.; Bougis, P. E.; Marchot, P. Conformational Flexibility of the Acetylcholinesterase Tetramer Suggested by X-Ray Crystallography *. *J. Biol. Chem.* **1999**, *274*, 30370−30376.
(36) Yang, H.; Yang, S.; Kong, J.; Dong, A.; Yu, S. Obtaining information about protein secondary structures in aqueous solution using Fourier transform IR spectroscopy. *Nat. Protoc.* **2015**, *10*, 382−396.
(37) Oliverio, R.; Liberelle, B.; Murschel, F.; Garcia-Ac, A.; Banquy, X.; De Crescenzo, G. Versatile and High-Throughput Strategy for the Quantification of Proteins Bound to Nanoparticles. *ACS Appl. Nano Mater.* **2020**, *3*, 10497−10507.
(38) Micsonai, A.; Wien, F.; Bulyáki, É.; Kun, J.; Moussong, É.; Lee, Y.-H.; Goto, Y.; Réfrégiers, M.; Kardos, J. BeStSel: a web server for accurate protein secondary structure prediction and fold recognition from the circular dichroism spectra. *Nucleic Acids Res.* **2018**, *46*, W315−W322.
(39) Kozlowski, R.; Ragupathi, A.; Dyer, R. B. Characterizing the Surface Coverage of Protein − Gold Nanoparticle Bioconjugates. *Bioconjugate Chem.* **2018**, *29*, 2691−2700.
(40) Liu, S.; Horak, J.; Höldrich, M.; Lämmerhofer, M. Accurate and Reliable Quantification of the Protein Surface Coverage on Protein-Functionalized Nanoparticles. *Anal. Chim. Acta* **2017**, *989*, 29−37.
(41) Filbrun, S. L.; Driskell, J. D. A fluorescence-based method to directly quantify antibodies immobilized on gold nanoparticles. *Analyst* **2016**, *141*, 3851−3857.
(42) Belsey, N. A.; Shard, A. G.; Minelli, C. Analysis of Protein Coatings on Gold Nanoparticles by XPS and Liquid-Based Particle Sizing Techniques. *Biointerphases* **2015**, *10*, No. 019012.
(43) Shang, W.; Nuffer, J. H.; Muñiz-Papandrea, V. A.; Colón, W.; Siegel, R. W.; Dordick, J. S. Cytochrome c on Silica Nanoparticles: Influence of Nanoparticle Size on Protein Structure, Stability, and Activity. *Small* **2009**, *5*, 470−476.
(44) Lundqvist, M.; Sethson, I.; Jonsson, B.-H. Protein Adsorption onto Silica Nanoparticles: Conformational Changes Depend on the Particles' Curvature and the Protein Stability. *Langmuir* **2004**, *20*, 10639−10647.
(45) Wang, A.; Vo, T.; Le, V.; Fitzkee, N. C. Using Hydrogen − Deuterium Exchange to Monitor Protein Structure in the Presence of Gold Nanoparticles. *J. Phys. Chem. B* **2014**, *118*, 14148−14156.
(46) Kelly, S. M.; Jess, T. J.; Price, N. C. How to Study Proteins by Circular Dichroism. *Biochim. Biophys. Acta, Proteins Proteomics* **2005**, *1751*, 119−139.
(47) Greenfield, N. J. Using Circular Dichroism Spectra to Estimate Protein Secondary Structure. *Nat. Protoc.* **2006**, *1*, 2876−2890.
(48) Shimizu, M.; Kobayashi, K.; Morii, H.; Mitsui, K.; Knoll, W.; Nagamune, T. Secondary Structure Analyses of Protein Films on Gold Surfaces by Circular Dichroism. *Biochem. Biophys. Res. Commun.* **2003**, *310*, 606−611.
(49) Kranz, B.; Bürck, J.; Franzreb, M.; Köster, R.; Ulrich, A. S. Circular Dichroism Analysis of Penicillin G Acylase Covalently Immobilized on Silica Nanoparticles. *J. Colloid Interface Sci.* **2007**, *316*, 413−419.
(50) Yang, J. A.; Johnson, B. J.; Wu, S.; Woods, W. S.; George, J. M.; Murphy, C. J. Study of Wild-Type α - Synuclein Binding and Orientation on Gold Nanoparticles. *Langmuir* **2013**, *29*, 4603−4615.
(51) Micsonai, A.; Wien, F.; Kernya, L.; Lee, Y.; Goto, Y.; Réfrégiers, M.; Kardos, J. Accurate Secondary Structure Prediction and Fold Recognition for Circular Dichroism Spectroscopy. *Proc. Natl. Acad. Sci. U. S. A.* **2015**, *112*, E3095−E3103.
(52) Ellman, G. L. Tissue Sulfhydryl Groups. *Arch. Biochem. Biophys.* **1959**, *82*, 70−77.
(53) Chan, M. S.; Landig, R.; Choi, J.; Zhou, H.; Liao, X.; Lukin, M. D.; Park, H.; Lo, P. K. Stepwise Ligand-Induced Self-Assembly for Facile Fabrication of Nanodiamond − Gold Nanoparticle Dimers via Noncovalent Biotin − Streptavidin Interactions. *Nano Lett.* **2019**, *19*, 2020−2026.
(54) Ye, L.; Pelton, R.; Brook, M. A. Biotinylation of TiO_2 Nanoparticles and Their Conjugation with Streptavidin. *Langmuir* **2007**, *23*, 5630−5637.
(55) Agarwal, P.; Bertozzi, C. R. Site-Specific Antibody − Drug Conjugates: The Nexus of Bioorthogonal Chemistry, Protein Engineering, and Drug Development. *Bioconjugate Chem.* **2015**, *26*, 176−192.
(56) Scino, S. L.; Bilodeau, D. A.; Hincapie, R.; Lee, W.; Nguyen, S. S.; Xu, M.; Am Ende, C. W.; Finn, M. G.; Lang, K.; Lin, Q.; Pezacki, J. P.; Prescher, J. A.; Robillard, M. S.; Fox, J. M. Bioorthogonal Chemistry. *Nat. Rev. Methods Primers* **2021**, *1*, 30.
(57) Ceylan, H. A. M. İ. D.; An, O. E. Ğ. Cloning, Expression, and Characterization of Human Brain Acetylcholinesterase in Escherichia Coli Using a SUMO Fusion Tag. *Turk. J. Biol.* **2017**, *41*, 77−87.
(58) Xiong, S.; Deng, Y.; Zhou, Y.; Gong, D.; Xu, Y.; Yang, L.; Chen, H.; Chen, L.; Song, T.; Luo, A.; Deng, X.; Zhang, C.; Jiang, Z. Current Progress in Biosensors for Organophosphorus Pesticides Based on Enzyme Functionalized Nanostructures: A Review. *Anal. Methods* **2018**, *10*, 5468−5479.
(59) Yang, Y.; Asiri, A. M.; Du, D.; Lin, Y. Acetylcholinesterase Biosensor Based on a Gold Nanoparticle-Polypyrrole-Reduced Graphene Oxide Nanocomposite Modified Electrode for the Amperometric Detection of Organophosphorus Pesticides. *Analyst* **2014**, *139*, 3055−3060.
(60) Luckham, R. E.; Brennan, J. D. Bioactive Paper Dipstick Sensors for Acetylcholinesterase Inhibitors Based on Sol-Gel/Enzyme/Gold Nanoparticle Composites. *Analyst* **2010**, *135*, 2028−2035.
(61) Niday, E.; Wang, C.-S.; Alaupovic, P. Kinetic Evidence for the Allosteric Substrate Inhibition of Human Erythrocyte Acetylcholinesterase. *Biochim. Biophys. Acta* **1980**, *612*, 67−72.
(62) Johnson, K. A.; Goody, R. S. The Original Michaelis Constant: Translation of the 1913 Michaelis-Menten Paper. *Biochemistry* **2011**, 8264−8269.
(63) Silman, I.; Sussman, J. L. Acetylcholinesterase: How Is Structure Related to Function ? *Chem.-Biol. Interact.* **2008**, *175*, 3−10.
(64) Colletier, J.; Greenblatt, H. M.; Sussman, J. L.; Silman, I.; Weik, M. Structural Insights into Substrate Traffic and Inhibition in Acetylcholinesterase. *EMBO J.* **2006**, *25*, 2746−2756.
(65) Stojan, J.; Brochier, L.; Alies, C.; Colletier, J. P.; Fournier, D. Inhibition of Drosophila Melanogaster Acetylcholinesterase by High Concentrations of Substrate. *Eur. J. Biochem.* **2004**, *271*, 1364−1371.
(66) Johnson, J. L.; Cusack, B.; Davies, M. P.; Fauq, A.; Rosenberry, T. L. Unmasking Tandem Site Interaction in Human Acetylcholinesterase. Substrate Activation with a Cationic Acetanilide Substrate †. *Biochemistry* **2003**, *42*, 5438−5452.
(67) Zhang, L.; Hu, D.; Salmain, M.; Liedberg, B.; Boujday, S. Direct Quantification of Surface Coverage of Antibody in IgG-Gold Nanoparticles Conjugates. *Talanta* **2019**, *204*, 875−881.
(68) Gittins, D. I.; Caruso, F. Spontaneous Phase Transfer of Nanoparticulate Metals from Organic to Aqueous Media. *Angew. Chem., Int. Ed.* **2001**, *40*, 3001−3004.
(69) Liu, X.; Atwater, M.; Wang, J.; Huo, Q. Extinction Coefficient of Gold Nanoparticles with Different Sizes and Different Capping Ligands. *Colloids Surf., B* **2007**, *58*, 3−7.

https://doi.org/10.1021/acsabm.2c00834
ACS Appl. Bio Mater. 2023, 6, 209−217